Food Hydrocolloids 174 (2026) 112405

Contents lists available at ScienceDirect

Food Hydrocolloids

journal homepage: www.elsevier.com/locate/foodhyd

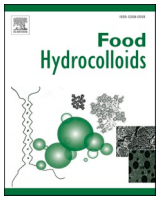

Covalent protein-phenolic modification – Effect of the phenolic compound structure on protein modification and conformational changes

Solange M.L. Ha [a,b], Kerstin Schild [a,c], Timon R. Heyn [c], Anna-Kristina Marel [d], Karin Schwarz [c], Wouter J.C. de Bruijn [b], Julia K. Keppler [a,*]

[a] Laboratory of Food Process Engineering, Wageningen University & Research, Bornse Weilanden 9, 6708 WG, Wageningen, the Netherlands
[b] Laboratory of Food Chemistry, Wageningen University & Research, Bornse Weilanden 9, 6708 WG, Wageningen, the Netherlands
[c] Christian-Albrechts-University of Kiel, Institute of Human Nutrition and Food Science, Division of Food Technology, Heinrich-Hecht Platz 10, 24118, Kiel, Germany
[d] Department of Food Technology and Bioprocess Engineering, Max Rubner-Institute, Federal Research Institute of Nutrition and Food, 76131, Karlsruhe, Germany

ARTICLE INFO

Keywords:
Phenolic compound modification
Structure-function analysis
Protein-polyphenol interaction
Hydroxycinnamic acid and derivatives
Flavonoids
Benzoic acid and derivatives

ABSTRACT

Phenolic compounds can undergo auto-oxidation, especially at alkaline pH, forming reactive *o*-quinones that bind covalently to proteins and may affect the protein structure, solubility, and functional properties. Yet, it is still unclear how the phenolic compounds' structure and properties affect their reaction with proteins, and how they influence the resulting changes in protein structure and functionality. Therefore, the model protein β-lactoglobulin (BLG) was incubated with ten common phenolic compounds at pH 8.5 for 24 h at a phenolic-to-protein molar ratio of 5:1. RP-HPLC was used to screen for covalent modifications. Protein structural changes were investigated using MALDI-TOF-MS, OPA and Ellman's assays, ATR-FTIR, tryptophan fluorescence quenching, SDS-PAGE, and SEC. Protein functionality changes were determined by oil droplet size measurement after emulsion formation via high pressure homogenization.

Only phenolic compounds with a di or-trihydroxybenzene moiety resulted in noteworthy BLG modification (>40 %), with an average of one phenolic compound bound per protein molecule, primarily on the thiol groups of the cysteine residues. Modification decreased the protein's α-helices and shifted the intramolecular β-sheets to higher wavelengths. Protein modification resulted in the formation of smaller oil droplets (from 1.38 to 2 μm) at low homogenization pressure. A positive relationship was found between the presence of a carboxyl group in the phenolic compounds, the unfolding of the protein's tertiary structure ($R^2 = 0.95$), and smaller oil droplet size. The insights from this study support the selection of phenolic compounds for targeted protein modifications or for avoiding undesired protein modifications.

1. Introduction

Phenolic compounds are secondary metabolites naturally present in plants, where they serve a wide variety of functions (Cheynier, 2012; Zhang et al., 2021). During food processing and storage, phenolic compounds can be oxidized, either enzymatically or via auto-oxidation, to radical semi-quinones and *ortho*-quinones. Auto-oxidation of phenolic compounds primarily spontaneously occurs at alkaline conditions, such as those used during protein isolation (Kieserling et al., 2024). The resulting electron-deficient semi- or *o*-quinones can participate in oxidative coupling reactions between phenolic compounds themselves and with nucleophilic side chains of amino acid residues in proteins, such as the amino group of lysine or thiol group of cysteine, leading to covalent modification of proteins (Drucker et al., 2023; Kieserling et al., 2024). These reactions in turn affect the proteins' structure, solubility, and functional properties (Cheynier, 2012; Rawel et al., 2001; Tanger et al., 2020; Zhang et al., 2021). On the one hand, uncontrolled reactions can be undesired due to negative effects on protein functionality, such as reduction in solubility or digestibility (Kieserling et al., 2024). On the other hand, there are also opportunities to exploit these reactions for targeted modification of proteins to enhance their properties as food ingredients (Keppler et al., 2020).

For the purpose of targeted modification of proteins, one of the open research questions is to understand the relationships between the structure of the phenolic compound and its ability to modify a protein, as well as the effect of this modification on the protein structure and

* Corresponding author. Wageningen University & Research, Bornse Weilanden 9, 6708 WG, Wageningen, the Netherlands.
E-mail address: Julia.keppler@wur.nl (J.K. Keppler).

https://doi.org/10.1016/j.foodhyd.2025.112405
Received 13 November 2025; Received in revised form 17 December 2025; Accepted 24 December 2025
Available online 26 December 2025

functionality. Establishing such relationships would allow a more targeted selection of phenolic compounds to achieve the desired protein modifications.

With respect to phenolic compounds, it is well known that covalent protein-phenolic reactions are *o*-quinone mediated. It is, therefore, assumed that the parent phenolic compound should contain a 1,2-dihydroxybenzene (catechol) moiety to enable protein modification. Nevertheless, there are reports that phenolic compounds with only one hydroxyl group instead of one or two methoxy groups, such as ferulic acid and sinapic acid, can also modify proteins under specific conditions (Condict et al., 2019; Kallinich et al., 2018). Furthermore, recent reviews have summarized that the structure of phenolic compounds—and their resulting chemical and physical properties such as molecular weight and, hydrophobicity—influence their reactivity toward proteins (Masoumi et al., 2024; Ozdal et al., 2013). We hypothesize that, besides the structure of the phenolic compound, its ability to modify proteins and the resulting effect on the protein structure and functionality will be dictated by the phenolic compounds' properties such as molecular weight, volume, and pK_a. However, systematic studies comparing a wide range of phenolic compounds under identical experimental conditions are still lacking. Thus, the aim of this study was to compare the extent to which ten phenolic compounds with varying structure and properties can covalently modify protein under uniform auto-oxidative conditions, and how this modification affects protein structure. To this end, we

Table 1
Phytochemical reference (i.e. allyl isothiocyanate) and phenolic compounds used for incubation with BLG with their molecular formulae, exact masses, van der Waals volume, pK_a, hydrophobicity, chemical structures, and PubChem CIDs.

Phytochemical	Molecular formula	Exact mass (Da)	Van der Waals volume (Å^3)[a]	pK_a[a]	Hydrophobicity (Log P)[a] (pH = 7)	Chemical structure	PubChem CID
Allyl isothiocyanate (AITC)	C_4H_5NS	99.01	129.716	14.0	1.314		5971
(−)-epicatechin (EC)	$C_{15}H_{14}O_6$	290.08	356.508	7.83	0.948	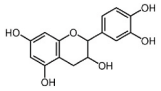	72276
Rutin	$C_{27}H_{30}O_{16}$	610.15	702.399	6.53	−1.003	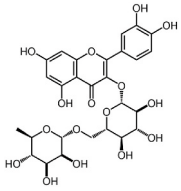	5280805
Caffeic acid (CA)	$C_9H_8O_4$	180.04	223.001	5.40	0.966	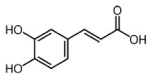	689043
Rosmarinic acid (RA)	$C_{18}H_{16}O_8$	360.08	440.147	4.03	1.847	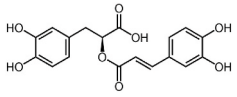	5281792
Chlorogenic acid (CGA)	$C_{16}H_{18}O_9$	354.10	417.516	4.30	−0.276	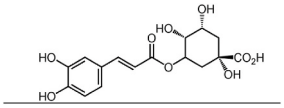	1794427
Gallic acid (GA)	$C_7H_6O_5$	170.02	188.567	5.33	−0.085	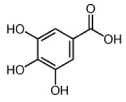	370
p-coumaric acid (pCA)	$C_9H_8O_3$	164.05	214.479	5.39	1.459	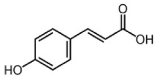	637542
Ferulic acid (FA)	$C_{10}H_{10}O_4$	194.06	249.570	5.42	1.385	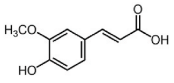	445858
Sinapic acid (SA)	$C_{11}H_{12}O_5$	224.07	284.660	5.44	1.327	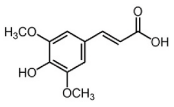	637775
Vanillic acid (VA)	$C_8H_8O_4$	168.04	206.613	5.48	0.806	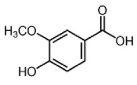	8468

[a] Values were computed using Molecular Operating Environment, v2024.0601 (Chemical Computing Group ULC., Montreal, Canada), using the method described by Kalli et al. (2022) (supplementary materials).

incubated the well-characterized model protein β-lactoglobulin (BLG) with ten common phenolic compound at alkaline conditions. We then analyzed whether BLG was covalently modified by these phenolic compounds and determined the effect of modification on protein microstructure (i.e. primary structures), mesostructure (i.e. secondary to quaternary structure), and macrostructure (i.e. emulsion formation).

2. Materials and methods

2.1. Materials

β-lactoglobulin (BLG) (PubChem CID: 142–148) (96 % protein on dry matter) was purchased from Davisco Foods International, Inc., (Le Sueur, MN, USA). The phytochemicals allyl isothiocyanate, rutin, gallic acid, ferulic acid, sinapic acid, and vanillic acid were purchased from Carl Roth GmbH + Co. KG (Karlsruhe, Germany). (−)-Epicatechin, caffeic acid, rosmarinic acid, chlorogenic acid, and p-coumaric acid were purchased from Sigma-Aldrich (St. Louis, MO, USA) (Table 1). All phytochemicals were of analytical purity (>95 %). *N*-acetyl-l-cysteine, borate buffer pH 9.3, urea, tris(hydroxymethyl)aminomethane, glycine, l-cysteine, methanol (≥99.9 %), ethanol (≥99.9 %), trifluoracetic acid (TFA), and acetonitrile (ACN) was also purchased from Carl Roth GmbH + Co. KG. Sodium hydroxide, l-leucine, sodium dodecyl sulphate (SDS), 5,5′-dithiobis(-2-nitrobenzoic) (DTNB), dithiothreitol (DTT), bovine serum albumin (BSA), and phosphate buffer containing $CaCl_2$ and $MgCl_2$ were purchased from Sigma-Aldrich. 1-Palmitoyl-2-oleoyl-glycero-3-phosphocholine (POPC) and 1,2-dipalmitoyl-snglycero-3-phosphoethanolamine-N- (cap biotinyl) (sodium salt) (biotin-PE) were obtained from Avanti Polar Lipids (Birmingham, Alabama, USA). Streptavidin was obtained from VWR International (Darmstadt, Germany). All water used was obtained from a Milli-Q water purification system (Merck). All other chemicals were used as received.

2.2. Phenolic compound set and sample preparation

The well-characterized model protein β-lactoglobulin (BLG) was incubated with ten common phenolic compounds differing in their structural features (hydroxyl and methoxy groups), molecular weight (99–610 Da), molecular volume (188–702 $Å^3$), and hydrophobicity (Log P −0.085 to 1.847) (Table 1). The compounds used are categorized as flavonoids ((−)-epicatechin and rutin, e.g. present in tea and grains), hydroxycinnamic acids & derivatives (caffeic, rosmarinic, chlorogenic, *p*-coumaric, ferulic, and sinapic acid; ubiquitously present in plant-derived foods), and benzoic acids & derivatives (gallic and vanillic acid; e.g. present in tea and nuts). The phytochemical allyl isothiocyanate (AITC), with its high binding capacity to BLG, was used as a reference compound, as the binding mechanisms is well-understood (Anantharamkrishnan & Reineccius, 2020; Keppler et al., 2017; Keppler et al., 2014). Covalent protein-phytochemical modification was induced at alkaline pH with a phytochemical-to-protein molar ratio of 5:1. BLG dispersed in water (0.5 mM) was incubated with phytochemical (2.5 mM in ethanol), with a final ethanol concentration of 2 % (*v/v*) to prevent protein denaturation. The pH of the protein-phytochemical mixtures was adjusted to 8.5 using NaOH and incubated for 24 h. During incubation the pH was re-adjusted with 4 M NaOH and the samples, with the exception of the AITC incubation, were exposed to atmospheric air to oxidize the phenolic compound. After incubation, the unbound phytochemicals were removed by ultrafiltration using an Amicon stirred cell (Merck KGaA, Darmstadt, Germany) and an Ultracel Membrane with 10 kDa cutoff (Merck KGaA). Afterwards, the samples were lyophilized for 72 h (Gamma 1–16 LSCplus, Martin Christ Gefriertrocknungsanlagen GmbH, Osterode, Germany) and were stored in airtight containers at −20 °C until further use. Additionally, a reference (BLG ref) was prepared following the same protocol, without the addition of a phytochemical. All samples were prepared in experimental triplicates. Following incubation, the proteins' microstructure (i.e. primary structure), mesostructure (i.e. secondary to quaternary structure, and macrostructure (i.e. emulsion formation) were assessed.

2.3. RP-HPLC screening for covalent modification

BLG ref, and BLG incubated with phytochemical were investigated for the presence of native BLG using RP-HPLC, according to Keppler, Sönnichsen, et al. (2014). Briefly, 20 μL of 0.1 % (*w/v*) BLG in water was injected in an Agilent 1100 Series HPLC equipped with a diode array detector and PLRP-S column (300 Å, 8 mm, 150 × 4.6 mm) (Agilent Technologies, Santa Clara, CA, USA), with a flow rate of 1.0 mL/min, column temperature of 40 °C, detection wavelength at 205 nm, and a gradient step of 35–38 % B (1–8 min), 38–42 % B (8–16 min), 42–46 % B (16–22 min), 46–100 % B (22–22.5 min), and 100-35 % B (23–23.5 min), with A 0.1 % (*v/v*) TFA in water and B 0.1 % (*v/v*) TFA in ACN. Each experimental triplicate was measured once. Peak areas for BLG B and A were calculated using Origin(Pro) v.2025 (OriginLab Corporation, Northampton. MA USA).

2.4. Characterization of changes in protein structure

The changes in protein primary structure were investigated using matrix-assisted laser desorption/ionization time-of-flight mass spectroscopy (MALDI-TOF-MS) and by measuring the free amino and thiol groups on the protein before and after incubation using *ortho*-phthaladehyde (OPA) assay and Ellman's assay, respectively. The protein secondary and tertiary structure was analyzed using attenuated-total-reflection Fourier-transform infrared spectroscopy (ATR-FTIR) and tryptophan fluorescence, respectively. Lastly, the quaternary structure was investigated through sodium dodecyl sulphate-polyacrylamide gel electrophoresis (SDS-PAGE), and size-exclusion chromatography (SEC).

2.4.1. Mass analysis using MALDI-TOF-MS

To investigate the number of bound phytochemicals, the mass of BLG, BLG ref, and BLG incubated with phytochemicals were determined using MALDI-TOF-MS. A matrix solution of 2.5 % (*w/v*) sinapic acid solution in 50 % (*v/v*) ACN and 0.1 % (*v/v*) TFA was used. Spots were prepared by mixing 1 μL of the matrix solution with 1 μL of 0.4 % (*w/v*) protein solution on a MTP 384 ground steel target plate (Bruker Daltonics, Billercia, MA, USA). Mass spectra (*m/z* 5–20,000) were obtained in linear mode with positive ionization using an ultrafleXtreme workstation equipped with a Smartbeam-II laser of 355 nm controlled by FlexControl 3.4 software (Bruker Daltonics). Spectra were collected with an ion source voltage of 20 kV. The system was calibrated using a ready to use protein standard I (Bruker Daltonics). Data processing was performed using Flex Analysis 3.4 (Bruker Daltonics). Each experimental triplicate was measured once.

2.4.2. Free amino groups using OPA assay

The amount of free amino groups before and after incubation was determined using *ortho*-phthaladehyde (OPA) assay, based on Keppler, Koudelka, Palani, Stuhldreier, et al. (2014). In short, 60 μL of 125 μM protein solution was mixed with 1320 μL 0.3 % *N*-acetyl L-cysteine in 0.1 M borate buffer pH 9.3 and 75 μL 20 % (*w/v*) SDS, followed by incubation at 50 °C for 10 min. After incubation, 45 μL of 3.4 % (*w/v*) OPA in methanol was added and the samples were further incubated at 50 °C for 30 min. Prior to measuring the samples at 340 nm (Helios γ, Thermo Fisher Scientific, Waltham, MA, USA), the samples were left to equilibrate at room temperature for 30 min. The measurements were corrected for the absorption effects of the phytochemicals itself by measuring the phytochemical solutions without protein. Each experimental triplicate was measured thrice. A calibration curve was made with L-leucine in the concentration range 2–120 μM.

2.4.3. Free thiol groups using Ellman's assay

The amount of free thiol groups before and after incubation with

phytochemical was determined according to Kehoe et al. (2007). Briefly, 200 μL of 125 μM protein solution was mixed with 800 μL 8 M urea in 50 mM Tris-glycine buffer pH 8.5. To this mixture 40 μL 10 mM DTNB in 50 mM Tris-glycine buffer pH 8.5 was added, followed by incubation at room temperature for 10 min. Samples were measured at 412 nm (Helios γ, Thermo Fisher Scientific) and corrected for the absorption effect of the phytochemicals. Each experimental triplicate was measured thrice. A calibration curve was made with L-cysteine in the concentration range 2.5–30 μM.

2.4.4. Protein secondary protein structure using ATR-FTIR

Protein folding was investigated using ATR-FTIR, based on Keppler et al. (2017). Protein solutions (2.5 % [*w/v*]) were measured on a Tensor 2 spectrometer equipped with a BioATR II Cell at 25 °C (Bruker Optics GmbH, Ettlingen, Germany) in the wavenumber range 4000 cm^{-1} to 900 cm^{-1}. An LN-MCT Photovoltaic detector (Bruker Optics) cooled with liquid nitrogen was used for detection. OPUS version 7.5 (Bruker Optics) was used to monitor and control the spectrometer and Ministat 125 thermostat (Huber, Offenburg, Germany), and to record the spectra. For each analysis, 120 scans were made at a resolution of 0.7 cm^{-1}. All samples were corrected using Milli-Q water. Each experimental triplicate was measured thrice. From the resulting spectra, the baseline was subtracted and vector normalized at the protein amide I region (1700-1600 cm^{-1}), followed by calculating the secondary derivatives using OPUS version 7.5. To compare the structural changes between samples, principal component analysis plots were made from the secondary derivative spectra using Origin(Pro) v.2025.

2.4.5. Protein tertiary structure using tryptophan fluorescence

Tryptophan fluorescence quenching was used to study the change in protein structure after modification. Protein solutions of 0.025 % (*w/v*) in 0.1 M HEPES (4-(2-hydroxyethyl)-1-piperazineethanesulfonic acid) buffer pH 7 were excited at 295 nm (slit 5 nm) while the emission was recorded over a wavelength range of 300–500 nm (slit 5 nm). The fluorescence intensities were measured at room temperature using a Varian Cary Eclipse right angle fluorescence spectrophotometer (Varian GmbH Darmstadt, Germany) and a quartz cuvette with four polished sides. The spectra were corrected with the HEPES buffer without protein. Each experimental triplicate was measured once. Origin(Pro) was used to calculate peak areas.

2.4.6. Molecular weight analysis using SDS-PAGE

Protein cross-linking was assessed by using sodium dodecyl sulphate-polyacrylamide gel electrophoresis (SDS-PAGE). Samples were dispersed at 0.2 % (*w/v*) in a 10 mM sodium phosphate buffer (pH 7) and diluted 1:1 with sample buffer containing 0.1 M DTT. Followed, by heating at 100 °C for 10 min and centrifugation at 14,000 × *g* for 1 min. The samples were loaded into gels (Mini-PROTEAN TGX stain-free precast gels, Bio-Rad Laboratories, Lunteren, The Netherlands) and separated on a Mini-PROTEAN tetra cell at 200 V. Protein bands were visualised with Bio-Safe Coomassie blue stain (Bio-Rad Laboratories) and the molecular weight of the bands were assigned based on a standard protein marker (Precision plus protein standards Dual colour). Scanning and analysis of the gels were performed with a densitometer (GS-900, Bio-Rad laboratories) and Image Lab software v6.0 (Bio-Rad laboratories), respectively. One experimental triplicate was measured once.

2.4.7. Molecular weight analysis using SEC

The change in molecular weight was assessed using SEC, based on the method of Delahaije et al. (2016). BLG, BLG ref, and BLG incubated with phytochemicals were dispersed in a 10 mM sodium phosphate buffer (pH 7) at a concentration of 0.2 % (*w/v*) and centrifuged at 14,500×*g* for 10 min. Samples (50 μL) were injected into an ÄKTA pure 25 equipped with a Superdex 75 Increase 10/300 GL column (Marlborough, MA, USA) and eluted with the same buffer at a flow rate of 0.5 mL/min. The UV absorbance at 214, 280, and 320 nm were measured to monitor the elution. The column was calibrated with blue dextran (2000 kDa), α-lactalbumin (14.2 kDa), β-lactoglobulin (36.6 kDa), ovalbumin (43.0 kDa), and BSA (66.5 kDa). Each experimental triplicate was measured once.

2.4.8. Protein binding to an aptamer using QCM-D

Quartz crystal microbalance with dissipation monitoring (QCM-D) measurements were conducted using a qCell T Q2 dual channel system with a peristaltic pump (3T analytik, Tuttlingen, Germany) with silicon dioxide-coated 10 MHz sensor crystals, according to Çanak-Ipek et al. (2025) and Görner et al. (2024). Briefly, the sensors were cleaned with alkaline SDS solution, Milli-Q water, and ethanol, followed by drying under nitrogen stream. Crystals were treated with plasma for 5 min at 100 W using a Zepto One Semi-automatic kHz system (Diener electronics, Ebhausen, Germany). Measurements were conducted at 37 °C with a flow rate of 75 μL/min. In order to mimic a physiological environment, a supported lipid bilayer (SLB) was used to immobilize the biotinylated Apt 356 (aptamer) via biotin-streptavidin interaction. This bilayer was formed by small unilamellar vesicles composed of biotin-PE and POPC in a ratio of 5:95 (*v/v*), at a concentration of 1 mg/mL in TRIS buffer. Streptavidin was dissolved in PBS at a concentration of 100 μg/mL and applied to the SLB. A 1 mg/mL BSA solution was used to minimize non-specific interactions. The aptamer was dissolved in 10 mM TRIS buffer pH 8 containing 0.1 % BSA at a concentration of 0.5 μM. Before adding to the sensor, the aptamer solutions were heated to 95 °C for 5 min and cooled to room temperature. Measurements were conducted at pH 3.5, which is below the isoelectric point of BLG, to minimize electrostatic repulsion between protein and aptamer. BLG ref and BLG incubated with AITC, EC, rutin, CA, CGA, FA, and SA were dissolved in phosphate buffer pH 3.5 at a concentration of 0.1 mg/mL. All buffers and reagents were tempered to 37 °C in a water bath before use, and the buffers were degassed in an ultrasonic bath. Incubation steps of streptavidin, Apt 356, and BLG were conducted without flow to reduce sample consumption. All binding events were observed in real-time. Each experimental triplicate was measured once in a two chamber system.

2.5. Change in emulsification properties

2.5.1. Emulsion preparation

BLG ref and BLG incubated with phytochemicals were dispersed in a 10 mM phosphate buffer (pH 7) at a concentration of 0.4 % (*w/v*) and checked for complete dissolution of the powder. These protein solutions were used to prepare emulsion with rapeseed oil in an oil-to-protein solution ratio of 1:9 (*v/v*). Pre-emulsions were prepared using an Ultraturrax (IKA, Staufen, Germany) at 19,000 RPM for 1 min. This was followed by processing at 200, 400, or 1000 bar in a low volume microfluidizer (LV1, Microfluidics, Westwood, MA, USA) equipped with a F12Y mixing chamber with an orifice of 75 μm, respectively. Each experimental triplicate sample was homogenized once.

2.5.2. Change in particle size distribution

The particle size distributions of the solubilized oil droplets were determined by static light scattering, using a particle size analyser (LA-950V2, Horiba, Retsch Technology GmbH, Haan, Germany), based on the method of Keppler and Schwarz (2017). In short, emulsions were dispersed in distilled water in the wet chamber until the R and B transmittances were within the range of 70–90 %. Measurements were performed using a refractive index of 1.45 for rapeseed oil particles and 1.33 for water. The mean value, as well as the 10th, 50th, and 90th percentiles of the particle size distribution were determined.

2.5.3. Oil droplet surface charge

The surface charge of the oil droplets was determined by measuring the zeta potential, using a Zetasizer Nano ZS instrument (Malvern

Instruments, Herrenberg, Germany). The emulsions were diluted in 10 mM phosphate buffer pH 7 to an oil concentration of 1 mg/mL.

2.5.4. Colour assessment of the emulsions

The colours of the emulsions were measured using the X-Rite colorimeter SP60 series (Grandville, MI, USA). The colours were expressed as L^* (lightness), a^* (red/green), and b^* (blue/yellow) values. The change in colour in comparison to BLG ref was calculated according to equation (1).

$$\Delta E^*_{ab} = \left[\left(L^* - L^*_0\right)^2 + \left(a^* - a^*_0\right)^2 + \left(b^* - b^*_0\right)^2\right]^{1/2} \quad \text{(eq. 1)}$$

where L^*_0, a^*_0, and b^*_0 are the values for BLG ref and L^*, a^*, and b^* are the values for the BLG incubated with phytochemicals. Each experimental replicate was measured in triplicate.

2.6. Statistics

Significance of differences was determined by ANOVA followed by Tukey's honest significant differences test using Origin(Pro) v.2025. Significance was defined as $p < 0.05$. Different superscript letters represent statistical differences.

3. Results

β-Lactoglobulin (BLG) was incubated with ten different phenolic compounds and one reference phytochemical at alkaline pH to induce phenolic compound oxidation and subsequent covalent reaction with the protein. BLG incubated under identical conditions without the addition of any phytochemical was used as a reference sample (BLG ref). First, the incubated proteins were screened for covalent modification using RP-HPLC. Next, the changes in protein micro- and mesostructure were investigated using various analytical methods. Lastly, the changes in protein macrostructure were investigated by studying the emulsification properties of the modified proteins.

3.1. Screening for covalent protein modification using RP-HPLC

The RP-HPLC chromatograms of BLG ref and BLG incubated with the phytochemicals are shown in Fig. 1. For the reference protein, which was incubated at pH 8.5 without the addition of phenolic compounds, two peaks were observed at 18.5 min and 20 min, which represent BLG B and A, respectively. This elution profile was comparable to what was previously reported by (Keppler et al., 2017) for BLG. Incubation of BLG with AITC (Fig. 1A) led to a complete loss of the original BLG peaks. This was also previously reported for BLG modified with AITC and proposed to be due to increased hydrophobicity of the modified protein (Keppler et al., 2017). Besides this, a decrease in peak area in RP-HPLC can also indicate the formation of protein aggregates that remain in the pellet or filter retentate during sample preparation and are not injected (Keppler et al., 2017; Sęczyk et al., 2019).

A complete loss of BLG peak area was also observed for the RA

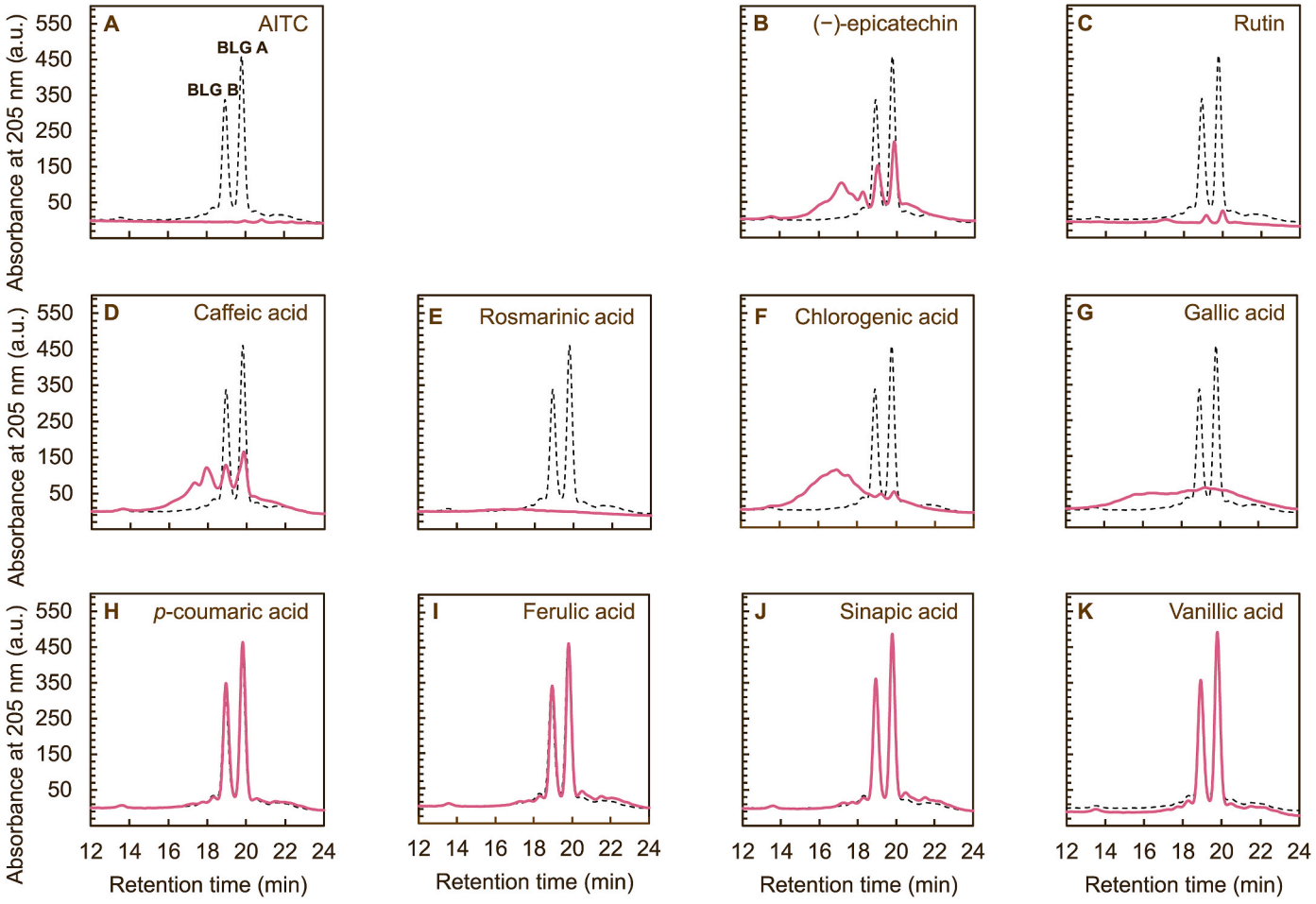

Fig. 1. RP-HPLC chromatograms of BLG ref (black dotted) and BLG incubated with allyl isothiocyanate (A), (−)-epicatechin (B), rutin (C), caffeic acid (D), rosmarinic acid (E), chlorogenic acid (F), gallic acid (G), *p*-coumaric acid (H), ferulic acid (I), sinapic acid (J), and vanillic acid (K) (pink solid). The plots presented are averages of experimental replicates ($n = 3$). a.u. = arbitrary units. (For interpretation of the references to colour in this figure legend, the reader is referred to the Web version of this article.)

(Fig. 1E) and GA (Fig. 1G) samples. Incubation with CA (Fig. 1D) and EC (Fig. 1B) led to a decrease of approximately 40 % in peak area (Table 3), whereas incubation with rutin (Fig. 1C) and CGA (Fig. 1F) led to a decrease of approximately 90 % and 80 % (Table 3), respectively. Incubation with pCA (Fig. 1H), FA (Fig. 1I), SA (Fig. 1J), and VA (Fig. 1K) did not lead to a significant decrease in BLG peak area, suggesting that no protein modification has taken place after 24 h incubation at pH 8.5.

Besides the decrease in peak area, a decrease in retention time was observed for EC, CA, and CGA, indicating decreased protein hydrophobicity. The attachment of phenolic compounds can alter the protein polarity due to blocking polar amino groups of proteins, inducing protein unfolding or by introducing polar hydroxyl and carboxyl groups (Ali et al., 2018). However, a comparison of the Log P values of the phenolic compounds (Table 1) revealed no clear relationship between their hydrophobicity before oxidation and the retention times of the modified protein. To obtain more in-depth insights into the protein modification, mass spectrometric analyses were conducted.

3.2. Change in protein primary structure upon incubation with phenolic compounds

3.2.1. Changes in protein mass

The change in protein mass after incubation with a phytochemical was measured using MALDI-TOF-MS (Fig. 2). The change in m/z relative to the reference protein is indicative for the number of bound phytochemicals. The reference protein had peaks at m/z of 18274 ± 6 and 18360 ± 6, representing BLG B and A, respectively. The change in mass was calculated by subtracting the measured m/z of BLG B or A and the exact mass (−2H) of n phytochemicals from the detected m/z value (Table A.1, supplementary materials). Based on these mass differences, the peaks were tentatively annotated as BLG B or A plus n phytochemicals. Besides the addition of the phytochemicals, a mixture of protonated, sodiated, and potassiated ions were observed in MALDI-TOF-MS.

For the reference compound AITC, up to five additions per protein molecule were found (Fig. 2A). Anantharamkrishnan and Reineccius (2020); Ersöz and Dudak (2020); Keppler, Koudelka, Palani, Tholey, et al. (2014); Rade-Kukic et al. (2011) found similar number of modifications for BLG with AITC. No unmodified protein was observed after incubation, which is in line with the results of the RP-HPLC analysis (Section 3.1).

The addition of at least one phenolic compound molecule to BLG B and A was identified for the flavonoids EC (Fig. 2B) and rutin (Fig. 2C), as well as for the hydroxycinnamic acid CA (Fig. 2D), its derivatives RA (Fig. 2E), and CGA (Fig. 2F). In line with the RP-HPLC results, the MALDI-TOF-MS results showed that incubation with EC, rutin, CA, or CGA resulted in extensive, but not complete, modification of BLG.

In the CA samples, three peaks were tentatively annotated: BLG A, BLG B + 1 CA, and BLG A + 1 CA (Fig. 2D). Two additional peaks could not be identified. Subtracting the mass of BLG B and 2 CA moieties for the first unidentified peak (*) resulted in a m/z of 34.2 ± 4.1 Da and subtracting BLG B and 3 CA moieties from the second unidentified (**) peak revealed a m/z of 36.4 ± 2.8 Da (Table A.1, supplementary

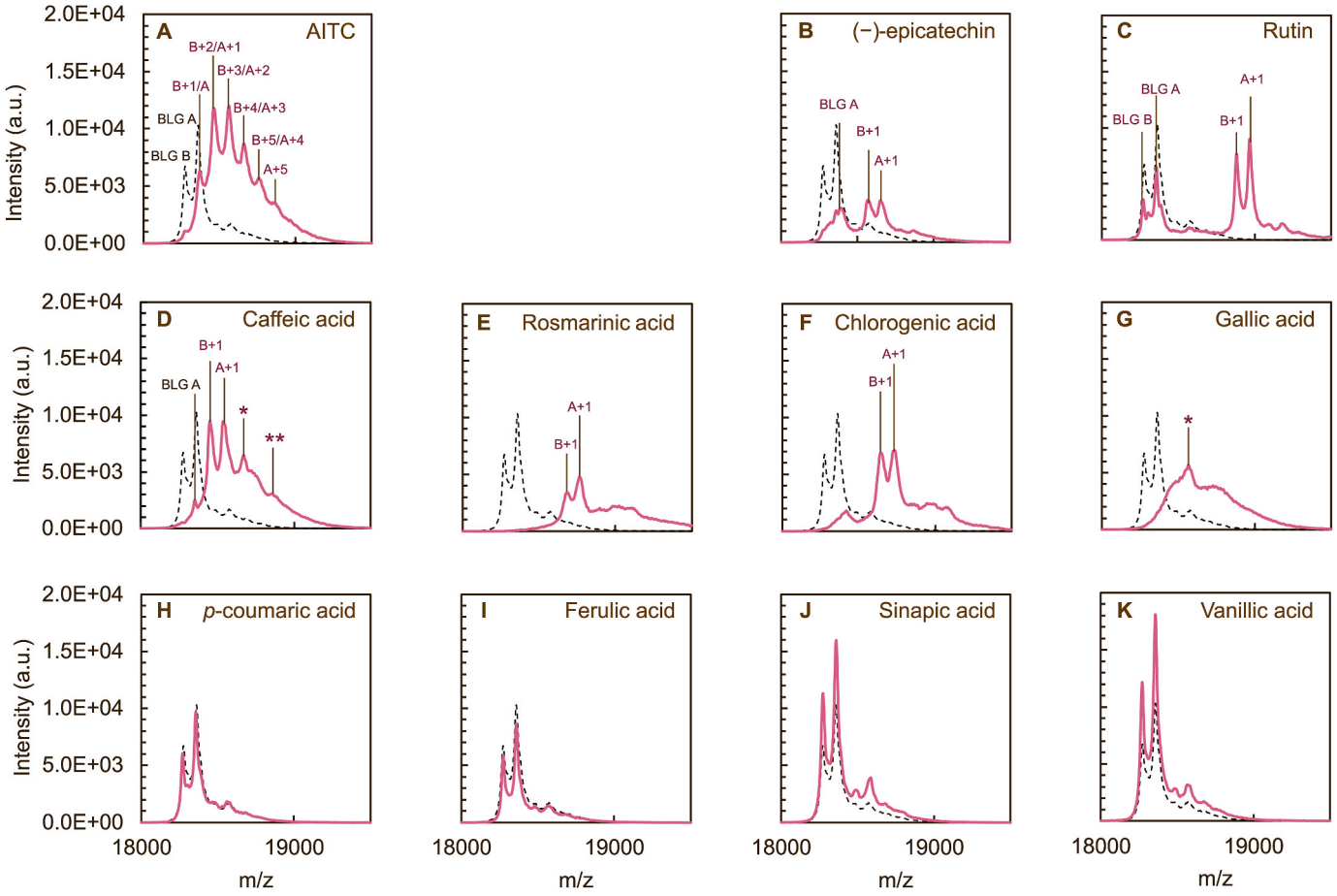

Fig. 2. MALDI-TOF-MS spectra with tentative annotations of BLG ref (black dotted) and BLG incubated with allyl isothiocyanate (A), (−)-epicatechin (B), rutin (C), caffeic acid (D), rosmarinic acid (E), chlorogenic acid (F), gallic acid (G), *p*-coumaric acid (H), ferulic acid (I), sinapic acid (J), and vanillic acid (K) (pink solid). The plots presented are averages of experimental replicates (n = 3), with * and ** indicating unknown compounds. a.u. = arbitrary units; A + n or B + n = number of phenolic compound molecule or AITC bound to BLG A or BLG B. (For interpretation of the references to colour in this figure legend, the reader is referred to the Web version of this article.)

materials). This residual mass detected could be due to formation of an unknown adduct during ionization. This indicates that 2 to 3 caffeic acid moieties were bound to the protein.

Similar results were observed for RA (Fig. 2E), where subtracting the mass of BLG B and A + 1 RA moiety, resulted in a residual mass of 46.3 ± 3.8 Da and 43.8 ± 1.6 Da in MALDI-TOF-MS (Table A.1, supplementary materials), which could be formation of an adduct during ionization. Besides these two peaks, there were additional peaks with residual masses larger than RA, but without a clear peak, indicating the modification of BLG with products resulting from RA undergoing further reactions (e.g. oxidation, degradation, or a combination thereof).

Like CA and RA, incubation of BLG with CGA resulted in the addition of 1 CGA per protein. In Fig. 2F, three peaks were observed. Two of the peaks detected in MALDI-TOF-MS were tentatively annotated as sodium

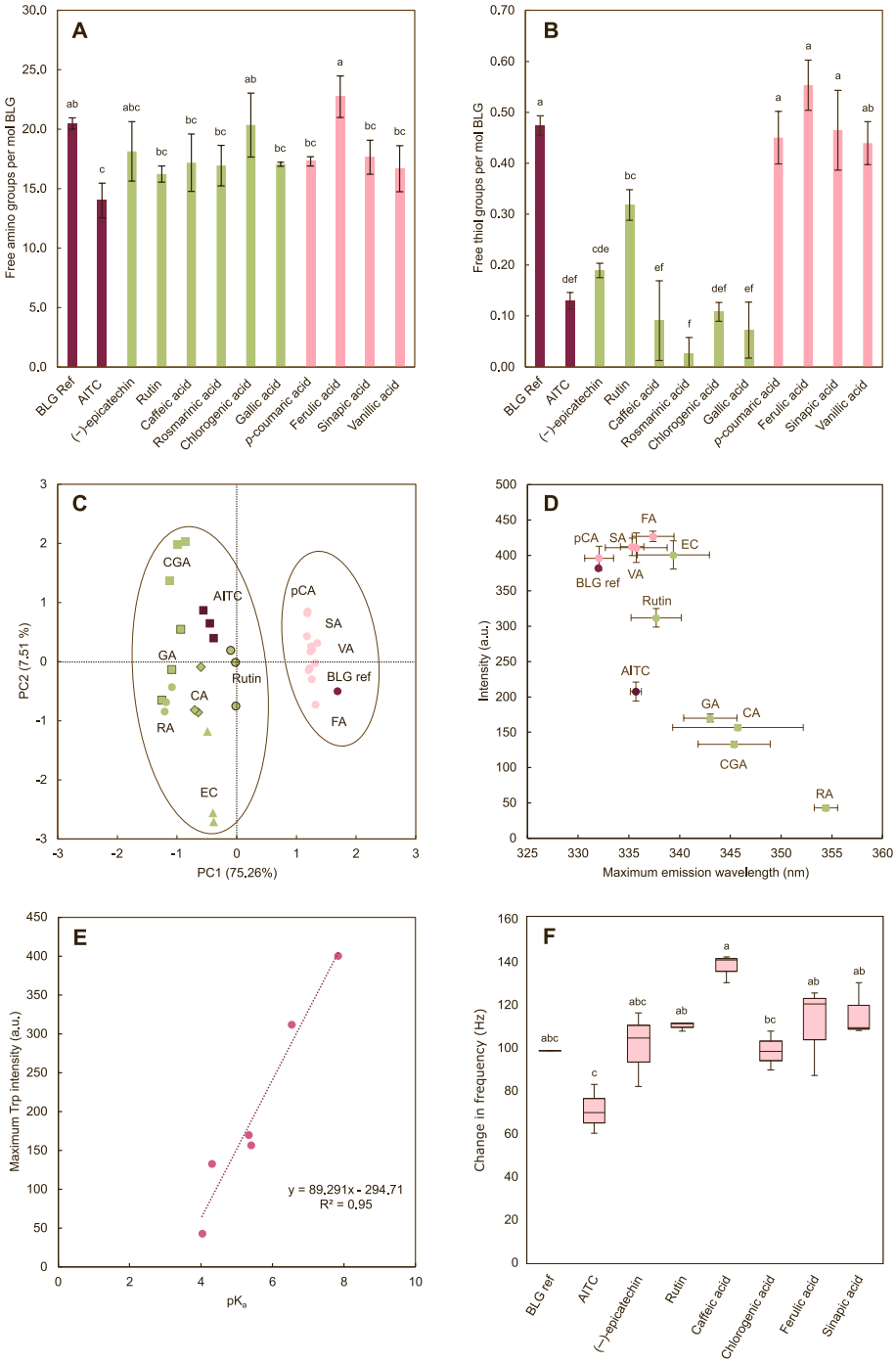

Fig. 3. Free amino groups (A), free thiol groups (B), principal component analysis plots of ATR-FTIR spectra (C), tryptophan fluorescence intensity at the maximum emission wavelength (D), tryptophan fluorescence at the maximum emission wavelength against the pK_a values of the phenolic compounds (E), and change in frequency due to interaction between BLG and the immobilized Apt 365 as measured using quartz crystal microbalance with dissipation monitoring (F) of BLG ref and BLG incubated with allyl isothiocyanate (AITC), (−)-epicatechin (EC), rutin, caffeic acid (CA), rosmarinic acid (RA), chlorogenic acid (CGA), gallic acid (GA), *p*-coumaric acid (pCA), ferulic acid (FA), sinapic acid (SA), and vanillic acid (VA). The average of each experimental replicate ($n = 3$) was plotted in A, B, and D, E, and F; C shows all replicates for each phenolic compound. Colours of bars or data points in A, B, C, and D represent: green, phenolic compounds that covalently modified BLG; light pink, phenolic compounds that did not modify BLG; and dark pink, BLG ref and the reference phytochemical AITC. a.u. = arbitrary units. (For interpretation of the references to colour in this figure legend, the reader is referred to the Web version of this article.)

adducts of BLG B and A with the addition of one CGA moiety (Table A.1, supplementary materials).

The benzoic acid derivative GA (Fig. 2G) showed an increase in protein mass between 100 and 600 *m/z*, which indicates the modification of BLG with GA products, similar to what was observed for RA. The other hydroxycinnamic acids pCA (Fig. 1H), FA (Fig. 1I), and SA (Fig. 1J), and the benzoic acid derivative VA (Fig. 1K) incubated with BLG did not show a change in mass in MALDI-TOF-MS, which is in accordance with the unchanged elution profiles observed by RP-HPLC.

3.2.2. Changes in free amino and thiol groups

To further investigate which amino acid side chains were conjugated with specific phenolic compounds, the free amino and thiol groups were determined after incubation (Fig. 3A and B). For BLG ref, 20.5 ± 0.47 free amino and 0.47 ± 0.02 free thiol groups were measured per mol protein, which is an overestimation of free amino groups (theoretical value = 16, with 15 lysines and the N-terminal amino group) and an underestimation of free thiol groups (theoretical value = 1, with 5 cysteines of which 4 are in disulphide bridges). Nonetheless, the relative values can be used to qualitatively compare the changes in free amino and thiol groups. For our reference phytochemical, AITC, a decrease in both free amino and thiol groups was observed, indicating the binding of AITC to the lysine and cysteine side chains, which was also found by Keppler et al. (2017). For the phenolic compounds that did not result in BLG modification (i.e. pCA, FA, SA, and VA; section 3.1 and 3.2.1), the free amino and thiol groups were also not significantly different from BLG ref, thereby demonstrating that the results of these assays can be interpreted qualitatively. The phenolic compounds that resulted in BLG modification (i.e. EC, rutin, CA, RA, CGA, and GA; section 3.1 and 3.2.1) only led to a clear reduction in the free thiol groups of the modified proteins. These results indicated that the cysteine residues were the predominant phenolic compound binding sites on the protein.

3.3. Changes in protein secondary structure using ATR-FTIR

The effect of covalent protein-phenolic modifications on protein secondary structure was investigated using ATR-FTIR. Figure A.1 (supplementary materials) shows the ATR-FTIR spectra with the wavenumber ranges that correspond to specific protein structures. The covalently modified BLG, with the exception of BLG modified by rutin, had a decrease in α-helix signal, a shift towards higher wavenumbers of the intramolecular β-sheets, and a decrease in β-sheet and turns. BLG modified with rutin mainly showed a decrease in α-helices and a minor decrease in intramolecular β-sheets. Although, similar findings were observed by Deng et al. (2023) and Pu et al. (2023) for BLG that was covalently modified with other phenolic compounds. The observed minor decrease in intramolecular β-sheets could be attributed to the lower extent of modification of BLG after incubation with rutin, as observed in MALDI-TOF-MS and the Ellman's assay (section 3.2).

To compare the changes in protein secondary structure, a principal component analysis was performed on the second derivative of the ATR-FTIR spectra of the amide I region (Fig. 3C). Two distinct clusters were formed, the first containing all modified proteins (green data points) and the second containing all unmodified proteins (pink data points). This difference was traced back primarily to the inter- (1600-1605 cm^{-1}, positive side) and intramolecular (1623-1628 cm^{-1}, negative side) β-sheets, based on the loading table (Table B.1, supplementary materials).

3.4. Change in protein tertiary structure using tryptophan fluorescence

To further investigate the changes in protein structure, tryptophan (Trp) fluorescence of the proteins was measured. An increase in maximum wavelength (λ_{max}), i.e. a red shift, indicates a more polar environment, whereas a decrease in λ_{max}, i.e. a blue shift, indicates a more apolar environment of the Trp in the incubated protein compared to the unmodified protein (Anantharamkrishnan & Reineccius, 2020). The observed maximum emission wavelengths and intensities for BLG ref and BLG incubated with phytochemicals are presented in Fig. 3D. The full emission spectra are presented in Figure A.2 (supplementary materials). BLG incubated with EC and rutin showed similar spectra as BLG ref, with rutin having a 15 % lower intensity (Table 3). BLG modified by CA, RA, CGA, and GA showed a decreased fluorescence intensity as well as a red shift, indicating changes in protein folding. Comparing the pK_a values and the change in fluorescence intensity of the other phenolic compounds that modified the protein, it seems that with decreasing pK_a values, the fluorescence intensity decreases and is more red shifted. Fig. 3E shows the fluorescence intensity of the modified protein against the pK_a of the respective phenolic compound, resulting in a R^2 of 0.95.

3.5. Changes in protein quaternary structure

The change in quaternary structure was investigated using SDS-PAGE and SEC. Electrophoretic profiles, as shown in Figure A.3 (supplementary materials), did not show extensive protein cross-linking, as the top of the wells did not show a prominent protein band. In general, the band at ~18 kDa, representing BLG, was observed for all samples. Additionally, a band at ~36 kDA, which represents a covalent dimer of BLG (Rawel et al., 2001), was observed for all samples. The intensity of the dimeric protein band differs between the samples, with EC, RA, and GA showing more intense dimer bands. This indicates a shift in ratio between monomeric and dimeric protein. This same shift in ratio was also observed in SEC (Figure A.4, supplementary materials). Two peaks were observed at a column volume of 9 and 11, representing BLG dimer and monomer, respectively. The protein incubated with EC, RA, and GA showed the monomeric peak shifting towards lower column volumes and thus higher molecular weights.

3.6. Changes in protein aptamer binding capacity

QCM-D measurements were performed to investigate the binding capacity of BLG and modified BLG to the aptamer 365, which was selected due to its known binding of native BLG (Çanak-Ipek et al., 2025). That means that the aptamer has the capacity to bind to the native protein, but any changes induced by covalent modification of BLG, such as blocking of binding sites, conformation changes, or charge changes, may affect the capacity to interact with the aptamer in a positive or negative manner. In Fig. 3F the change in frequency, caused by the interaction of BLG with the immobilized aptamer, is presented for a selection of BLG samples that were substantially modified (based on the RP-HPLC results, Fig. 1) such as AITC, EC, Rutin, CA, and CGA, but also a selection of unmodified samples (reference, FA and SA). The protein modified with the reference compound AITC showed a decrease in frequency shift, indicating less interaction with the aptamer. In the case of BLG modified with CA, an increase in frequency shift was observed, which indicates strong interaction with the aptamer. For all other measured samples, minimal frequency differences were observed, indicating no significant changes in the capacity to interact with the aptamer.

3.7. Properties as emulsifier

To investigate the effect of covalent modification, the protein properties as emulsifiers were investigated. Emulsions were prepared at three homogenization pressures. A pressure of 200 bar, representative of industrial conditions, produced relatively unstable emulsions, allowing differences between differently modified proteins to be more clearly observed. Higher pressures of 400 and 1000 bar were applied to examine at which pressure protein structural effects are overridden by the homogenization conditions. The medians of the oil droplet size in all samples are presented in Fig. 4 and the particle size distribution can be

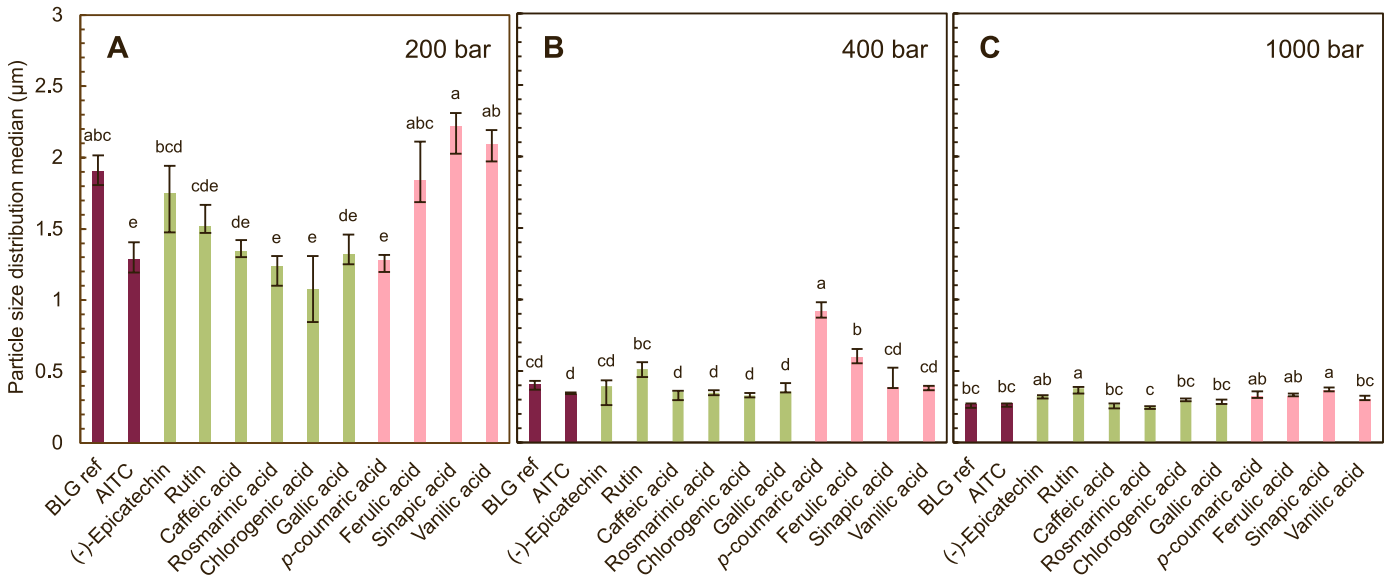

Fig. 4. Median particle size distribution of emulsions formed using rapeseed oil and BLG ref or BLG incubated with allyl isothiocyanate (AITC), (−)-epicatechin, rutin, caffeic acid, rosmarinic acid, chlorogenic acid, gallic acid, *p*-coumaric acid, ferulic acid, sinapic acid, and vanillic acid at a homogenization pressure of 200 (A), 400 (B), and 1000 (C) bar. Values are presented as averages and standard deviations of experimental replicates ($n = 3$), with different superscript letters representing statistical difference ($p < 0.05$). Colours of bars represent: green, phenolic compounds that covalently modified BLG; light pink, phenolic compounds that did not modify BLG; and dark pink, BLG ref and the reference phytochemical AITC. (For interpretation of the references to colour in this figure legend, the reader is referred to the Web version of this article.)

found in Figure A.5 (supplementary materials). Emulsion preparation at a pressure of 200 bar resulted in a particle diameter of approximately 2 μm. Protein modified with AITC, CA, RA, CGA, GA, and BLG incubated with pCA resulted in smaller oil droplet diameters between 1.3 and 1.7 μm. Increasing the pressure of the microfluidizer to 400 bar resulted in a polydisperse particle size distribution (Figure A.5, supplementary materials) with particle diameters of 0.3–1.0 μm. Although there were no significant differences in oil droplet size, the particle size distribution showed a smaller proportion of particles around 1 μm for BLG modified with AITC, EC, CA, RA, CGA, GA, and BLG incubated with VA compared to BLG ref. BLG modification with rutin and BLG incubated with pCA and FA showed a larger proportion of larger particles (>1 μm) than BLG ref. Increasing the pressure of the microfluidizer to 1000 bar, resulted in a predominantly monodisperse particle size distribution around 0.3 μm for all samples.

To identify the influence of charge on the emulsion stability, the zeta potential of all emulsions was examined (Table A.2, supplementary materials). However, no clear correlation could be established between the zeta potential and the measured particle size.

The resulting colours of the emulsion are presented in Figure A.6 (supplementary materials), with the colour difference expressed as ΔE^*_{ab} (−) presented in Table 2. Most ΔE^*_{ab} values were below 5, indicating that colour differences are not noticeable in most samples. Emulsions stabilized with protein modified with RA, CGA, or GA, showed ΔE^*_{ab} values between 5 and 10, indicating that colour differences could be perceptible through close observation.

4. Discussion

4.1. Microstructure

Based on the results described in Sections 3.1 and 3.2, and Tables 3 and it can be confirmed that the structure of phenolic compounds influences their ability to covalently modify the protein. Only phenolic compounds containing a 1,2-dihydroxybenzene (i.e. EC, rutin, CA, RA, CGA) or 1,2,3-trihydroxybenzene (i.e. GA) moiety covalently modified the protein under these conditions, whereas phenolic compounds lacking these moieties (i.e. pCA, FA, SA, and VA) did not covalently modify BLG. Current literature regarding protein-phenolic reactions with pCA, FA, SA, and VA are either limited or show discrepancies in results. For example, similar to our results, Rawel et al. (2001) did not observe covalent modification of whey protein with FA after incubation at pH 9, which was confirmed with MALDI-TOF-MS, while Xue et al. (2023) have indicated covalent modification of BLG with FA after incubation at pH 9

Table 2
Colour difference between emulsion prepared using rapeseed oil and BLG incubated with phytochemicals in comparison to BLG ref. Values are reported as averages and standard deviations of biological replicates ($n = 3$) and are expressed as ΔE^*_{ab} (−). A ΔE^*_{ab} value above 3 indicates a colour difference perceptible through close observation and values above 10 indicate that the colours are more similar to the opposite. Different superscript letters represent statistical difference differences between samples within the same row ($p < 0.05$).

	ΔE^*_{ab} (−) in comparison to BLG ref										
	AITC	(−)-epicatechin	Rutin	Caffeic acid	Rosmarinic acid	Chlorogenic acid	Gallic acid	*p*-coumaric acid	Ferulic acid	Sinapinic acid	Vanillic acid
200 bar	2.8 ± 0.33 ^{de}	4.2 ± 0.39 ^{bc}	3.7 ± 0.02 ^{cde}	2.2 ± 0.25 ^{e}	5.9 ± 0.54 ^{a}	3.1 ± 0.36 ^{cde}	5.2 ± 0.33 ^{ab}	2.9 ± 0.60 ^{de}	2.7 ± 0.54 ^{de}	2.6 ± 0.40 ^{de}	3.0 ± 0.37 ^{cde}
400 bar	0.5 ± 0.50 ^{c}	3.3 ± 0.65 ^{b}	2.9 ± 0.17 ^{b}	3.2 ± 0.58 ^{b}	6.4 ± 0.24 ^{a}	6.2 ± 0.46 ^{a}	6.1 ± 0.61 ^{a}	0.5 ± 0.18 ^{c}	0.4 ± 0.07 ^{c}	0.7 ± 0.20 ^{c}	0.5 ± 0.33 ^{c}
1000 bar	0.7 ± 0.36 ^{d}	3.0 ± 0.45 ^{c}	3.1 ± 0.85 ^{c}	3.9 ± 1.72 ^{bc}	6.3 ± 0.13 ^{a}	5.3 ± 0.37 ^{ab}	5.8 ± 0.31 ^{ab}	0.5 ± 0.27 ^{d}	0.5 ± 0.11 ^{d}	0.8 ± 0.22 ^{d}	0.7 ± 0.29 ^{d}

Table 3
Summary of protein structural changes upon incubation of BLG with allyl isothiocyanate (AITC), (−)-epicatechin, rutin, caffeic acid, rosmarinic acid, chlorogenic acid, gallic acid, *p*-coumaric acid, ferulic acid, sinapic acid, and vanillic acid.

Phytochemical	Micro			Meso				Macro
	Relative decrease in BLG peak area as determined by RP-HPLC (%) [a]		Primary structure Number of bound phytochemicals per protein by MALDI-TOF-MS	Secondary structure Qualitative changes in protein secondary structure elements as determined by ATR-FTIR	Tertiary structure Relative decrease in fluorescence intensity (%) [b]	Quaternary structure SEC and SDS-PAGE	QCM-D Aptamer binding Relative change in frequency (%) [b]	Emulsion droplet reduction at 200 bar (μm)
	BLG B	BLG A						
AITC	103.5 ± 0.5	102.5 ± 0.9	5	α-helix & intramolecular β-sheet	45.1 ± 3.2	No changes	−28.1 ± 11.56	−0.6
(−)-Epicatechin	43.3 ± 5.5	43.1 ± 2.5	1	α-helix & intramolecular β-sheet	−11.6 ± 4.7	Dimer increase	2.4 ± 17.67	0
Rutin	89.3 ± 0.3	89.3 ± 0.8	1	α-helix	15.4 ± 4.6	Dimer increase	11.8 ± 2.18	−0.4
Caffeic acid	42.2 ± 1.2	39.9 ± 0.5	2	α-helix & intramolecular β-sheet	50.4 ± 0.5	Dimer increase	39.8 ± 6.66	−0.5
Rosmarinic acid	100.4 ± 0.2	101.3 ± 0.4	≥1 [c]	α-helix & intramolecular β-sheet	88 ± 0.9	Dimer increase	n.d.[d]	−0.6
Chlorogenic acid	79.8 ± 2.2	80.3 ± 4.3	1	α-helix & intramolecular β-sheet	59.7 ± 1.4	Dimer increase	0 ± 9.24	−0.8
Gallic acid	~63.8 ± 7.6	~63.5 ± 5.5	≥1 [c]	α-helix & intramolecular β-sheet	51 ± 1.8	Dimer increase	n.d.[d]	−0.6
p-coumaric acid	−3.4 ± 13.8	−3 ± 10.7	0	No changes	−4 ± 4.7	No changes	n.d.	−0.6
Ferulic acid	0.2 ± 1.8	0.7 ± 1.7	0	No changes	−9.9 ± 2.7	No changes	12.6 ± 21.17	0
Sinapic acid	−2.5 ± 4.5	−3.6 ± 4	0	No changes	−13.9 ± 1	No changes	17.6 ± 12.7	0
Vanillic acid	0.9 ± 13.7	−2.0 ± 12	0	No changes	−8.5 ± 6.5	No changes	n.d.[d]	0

[a] Relative concentration were calculated by determining the peak areas of BLG B and A and comparing these to the reference sample. Values are reported as averages and standard deviations of experimental triplicates ($n = 3$) and are expressed as percentages.
[b] Values are reported as averages and standard deviations of experimental triplicates ($n = 3$) and are expressed as percentages.
[c] The exact number of bound phytochemicals could not be determined but was at least 1 per protein.
[d] Not determined.

but only measured with colorimetric assays.

Overall, MALDI-TOF-MS gave evidence that on average one phenolic compound was bound to the protein, except for CA, for which addition of at least two molecules was detected (Table 3, and Fig. 2 and Table A.1, supplementary materials). The main binding sites on the protein were the free thiol groups of the cysteine residues, which were preferred over the amino groups of lysine residues. This is in line with previous findings by Liu et al. (2024) and Lund (2021). At pH 8.5, the thiol group of cysteine (pK_a 8.14) is partially deprotonated, making it more nucleophilic, thereby increasing its reactivity with electron-deficient *o*-quinones compared to the fully protonated amino group of lysine (pK_a 10.67). The addition of one phenolic compound molecule per protein was also reported in previous studies of Deng et al. (2023) (BLG with rutin), Jia et al. (2022) (soy protein with rutin), Kanakis et al. (2011) (BLG with EC), Liu et al. (2016) (BLG with CGA), Stănciuc et al. (2020) (BLG with CA), Wang et al. (2024) (BLG with RA), and Ye et al. (2021) (soy protein with rutin). All of these studies used alkaline modification with phenolic-to-protein molar ratios between 1:0.05 and 35:1.

The extent of protein modification was dependent on the phenolic compound, as rutin, RA, CGA, and GA almost completely modified the proteins based on RP- HPLC as well as MALDI-TOF-MS (Figs. 1 and 2), while EC and CA samples still contained unmodified BLG. This may be due to a different extent of oxidation of the phenolic compound or differences in reactivity of the oxidized phenolic compound towards BLG, for example a different electronegativity (Pritchard & Skinner, 1955; Xu & Chen, 2011). It has been suggested that differences in pK_a values and molecular weights of the reactants will also affect the reactivity (Masoumi et al., 2024; Ozdal et al., 2013), as deprotonation of the phenolic compounds' hydroxyl group(s) facilitates oxidation of the compound. Nevertheless, we could not identify a clear correlation between pK_a and extent of protein modification. Similarly, neither the molecular weight nor volume of the phenolic compound showed a clear correlation with the extent of protein modification. However, it should be noted that our tested phenolic compounds' molecular weights and volumes are in a quite narrow range.

Previous research by Rawel et al. (2002) concluded that the reactivity of phenolic acids and flavonoids with soy proteins is dependent on the number of hydroxyl substituents and the positions of these groups. In that study, they also observed that GA modified soy proteins more extensively compared to CGA and CA.

Higher reactivity could also lead to polymerisation of the phenolic compound prior to or after reaction with the protein. Upon incubation of phenolic compounds at alkaline pH, reactive *o*-quinones can be formed, which can polymerize with phenolic compound monomers to form polymers such as dimers and trimers (Zhou et al., 2021). Additionally, phenolic compounds could form other oxidation and degradation products, such as caffeicins from caffeic acid (Cilliers & Singleton, 1991). In our study, we observed in MALDI-TOF-MS the addition of multiple unidentified masses for GA. The addition of unidentified masses was, to a lesser extent, also observed for CA, CGA, and RA, and was attributed to the attachment of phenolic compound oxidation and/or degradation products to the protein.

Besides the phenolic compound requiring an 1,2-dihydroxybenzene or 1,2,3-trihydroxybenzene moiety, there were no clear relationships between the phenolic compound properties and their modification of the protein's microstructure.

4.2. Mesostructure

Notably, all proteins modified with a catechol or pyrogallol moiety exhibited a distinct shift of the intramolecular β-sheets toward higher wavenumbers, as reflected in PC1, compared to the unmodified protein

(Fig. 3C). Such a decrease in β-sheets has been reported before by studies on various combinations of proteins and phenolic compounds: Kong et al. (2023), walnut protein with walnut pellicle phenolic extracts; Li et al. (2024), Tartary buckwheat protein with rutin and quercetin; Malik et al. (2016), sunflower protein with polyphenols; Pang et al. (2021), hemp seed protein with EGCG; Parolia et al. (2022), lentil protein with quercetin, rutin, and ellagic acid; Yan et al. (2022), soy protein isolate with GA. Such a decrease in β-sheets is associated with decreasing protein aggregation (Barth, 2007; Dong et al., 2000; Heyn et al., 2019). Similar results were observed for BLG after modification with AITC at pH 7 by Rade-Kukic et al. (2011) and was correlated to a disruption of non-covalent protein dimers. In contrast, our SEC results for the protein modified with phenolic compounds indicated either no change or a minor shift towards the dimeric protein after modification (Figure A.4, supplementary materials). However, this measurement did not distinguish between non-covalent and covalent dimers. The SDS-PAGE results (Figure A.3, supplementary materials) showed an increase in covalent dimers after modification with phenolic compounds, but no extensive protein cross-linking. While SEC and SDS-PAGE excluded extensive protein cross-linking towards larger aggregates, which may occur at higher extents of modification (Rohn, 2014), a disruption of non-covalent dimers cannot be excluded.

Another interesting finding is the high correlation between the pK_a of the phenolic compound used to modify the protein and the fluorescence quenching and red shifting intensity (Fig. 3E). This may indicate that the change in protein tertiary structure is dependent on the pK_a and, consequently, the charge of the phenolic compound. For example, the negative charge of an attached phenolic compound could lead to repulsion of similarly charged amino acids and thus partial opening of the tertiary structure. Another explanation could be that the binding of a charged compound at a cysteine residue close to tryptophan simply results in quenching of the tryptophan fluorescence and is not directly related to conformational changes. Finally, the extent of modification also plays a role, as EC has the highest amount of residual unmodified BLG compared to the other modified samples, thereby maintaining a proportion of the intrinsic fluorescence intensity. Various other studies report intrinsic fluorescence quenching and red shifting of the emission maximum after covalent phenolic compound addition, e.g. Rawel, Czajka, et al. (2002) for soy protein modified with CA, CGA, and GA. Nevertheless, such a direct correlation between pK_a/red shift and tertiary structure has not been reported before. In line with findings from other studies investigating various phenolic compounds, chlorogenic acid ($pK_a = 4.3$) induced stronger intrinsic Trp fluorescence quenching and a more pronounced red shift compared to gallic acid ($pK_a = 5.33$) upon modification of BLG at alkaline pH. Despite its higher pK_a of 7.68 (Muzolf-Panek et al., 2012), EGCG caused a fluorescence intensity shift comparable to that of gallic acid (Man et al., 2024). However, in their research, the phenolic-to-protein molar ratio differed between the phenolic compounds, resulting in higher modification for EGCG. It is important to note that the pK_a values reported in literature vary widely, depending on the method used for determination. In our study, we computed all values using consistent methodology. Therefore, to verify if the observed correlation between computed pK_a values and tertiary structure changes is valid, follow-up studies with phenolic compounds possessing an even wider range of experimentally determined pK_a values are necessary.

The changes in protein primary to quaternary structure after modification with phenolic compounds, were expected to also change the protein binding to an aptamer that was selected to bind to native BLG. Indeed, the reference phytochemical AITC (lowest interaction with the aptamer) and CA (highest interaction) affected the aptamer interaction with the protein, most likely due to blocking of binding sites or changes in the charge of the protein leading to attraction or repulsion (Görner et al., 2024; Çanak-Ipek et al., 2025). These results confirmed that the properties of these two samples were changed substantially after modification. In contrast, rutin already stood out as a phenolic compound that hardly affected the protein secondary (Figure A.1C, supplementary materials) or tertiary structure (Figure A.2C.). As expected, based on those results, it also did not affect the aptamer binding. However, aptamer binding was largely unchanged by EC, CA, or CGA, even though they modified the protein. Thus, the extent of protein modification could not be linked to changes in the binding of the aptamer.

Besides the effect of the pK_a of the phenolic compound on the tertiary structure of the modified protein, we found no correlations between phenolic compound structure and the modified protein's mesostructure. A limitation of these comparisons is that we can only consider the original structure of the phenolic compounds with their corresponding properties. Reactions of the phenolic compounds (e.g. oxidative coupling) prior to or after their reaction with the protein should be further investigated in follow-up studies. Possibly, relationships exist between the structures and properties of these (intermediate) reaction products and the changes in protein secondary structure.

4.3. Macrostructure

Low pressure homogenization (200 bar) was used to create unstable emulsions with large droplet sizes to investigate the differences in emulsifying behaviour between the modified proteins. With the exception of rutin and EC, covalent modification of BLG with phenolic compounds led to a reduction in oil droplet size. This observation aligns with previous findings reported by Li et al. (2023) (rice bran protein with (+)-catechin, and Yan et al. (2022) (soybean protein isolate with GA). The smaller droplet sizes were attributed to a higher flexibility of the modified protein due to partial opening the tertiary structure. Additionally, opening of the tertiary structure exposes the proteins' hydrophobic group making them more surface-active (Keppler et al. (2017), Keppler et al. (2024); Keppler and Schwarz (2017). Other studies that modified BLG with caffeic acid through chemical coupling using 1-Ethyl-3-(3-dimethylaminopropyl) carbodiimide and *N*-hydroxysuccinimide showed an increase in oil droplet size after modification (Abd El-Maksoud et al., 2018). However, these reagents induce the binding of the carboxyl group of the phenolic acid to amino groups of the protein, which is different from the autoxidation reaction in the current study.

Interestingly, emulsions prepared with EC and rutin showed no statistically significant deviation from BLG ref, despite protein modification. Our results indicated that the absence of a carboxyl group in EC and rutin led to reduced unfolding of the protein's tertiary structure compared to the other phenolic compounds (Section 4.2). This may explain the lack of effect on oil droplet size, as less exposure of hydrophobic area of the protein is associated with a lower surface activity (Schröder et al., 2017). At higher homogenization pressures of 400 and 1000 bar, smaller and more comparable droplet sizes were formed. An outlier is the sample of BLG incubated with pCA, at 200 and 400 bar. An explanation could be that despite ultrafiltration, not all free pCA was removed. This phenolic compound may have non-covalently interacted with the protein or adsorbed to the interface itself and thereby influenced the emulsification properties (Yan et al., 2024). At 1000 bar, most of these differences were no longer detectable, likely due to the high homogenization pressure masking the subtle difference by overriding the effect of protein modification.

4.4. Concluding remarks

The aim of this study was to systematically compare the extent to which phenolic compounds with varying structure and properties can covalently modify protein under uniform auto-oxidative conditions, and how this modification affects protein structure. In terms of the phenolic compound properties and their effects across the micro-, meso-, and macrostructure levels, two consistent trends emerged. Firstly, a catechol (i.e. 1,2-dihydroxybenzene) or pyrogallol (1,2,3-trihydroxybenzene) moiety appears to be necessary to modify the protein. Secondly, there is a positive relationship between the presence of a carboxyl group, the unfolding of the protein's tertiary structure, and improved emulsifying properties. No clear relationships were observed between the changes in protein secondary structure and the structural features of the phenolic compounds, such as van der Waals volume or hydrophobicity, although possible relationships may exist between intermediate reaction productions.

Despite observing no relationships between the changes in protein secondary structure and phenolic compound structural features, covalent modification of BLG with caffeic, rosmarinic, chlorogenic, and gallic acid resulted in smaller oil droplet sizes at a homogenization pressure of 200 bar. However, at a homogenization pressure of 1000 bar, the effects of the changed protein structure were overridden and no significant changes in emulsification properties were observed.

A limitation of our research is that we focused on the structure and properties of the original phenolic compounds, and that we did not study the structure and properties of their oxidation products. Additionally, a relatively low phenolic-to-protein of 5:1 was used, which may have contributed to the absence of more extensively modified proteins. Increasing the phenolic-to-protein molar ratio might result in more extensive protein modification, consequently leading to considerably different protein structural changes and properties.

Nonetheless, our findings offer evidence to support the selection of phenolic compounds for targeted protein modifications, such as for improving emulsion formation, while also identifying compounds unlikely to interact with the protein. The observed consistency in protein structural and functional changes across modification with structurally diverse phenolic compounds establishes protein–phenolic interactions as a potential tool for controllable functionality tuning. This opens the way for designing process-integrated strategies in which phenolic compounds are deliberately co-extracted or retained to enhance emulsifying performance in plant-based ingredients and emulsion-based foods.

CRediT authorship contribution statement

Solange M.L. Ha: Writing – original draft, Visualization, Methodology, Investigation, Formal analysis, Data curation, Conceptualization. **Kerstin Schild:** Methodology, Investigation, Formal analysis, Data curation, Conceptualization. **Timon R. Heyn:** Writing – original draft, Methodology, Investigation, Data curation. **Anna-Kristina Marel:** Writing – original draft, Project administration, Methodology, Data curation, Funding acquisition. **Karin Schwarz:** Writing – review & editing, Supervision. **Wouter J.C. de Bruijn:** Writing – review & editing, Supervision, Methodology, Conceptualization. **Julia K. Keppler:** Writing – review & editing, Supervision, Project administration, Methodology, Funding acquisition, Conceptualization.

Funding

This project was supported by funds from the Federal Ministry of Food and Agriculture (BMEL) based on a decision by the Parliament of the Federal Republic of Germany via the Federal Office for Agriculture and Food (BLE) under the Innovation Support Programme (FKZ 281A302B18).

The research was also performed as part of the "ProTip – Understanding protein-phenolic interaction: Tipping the scale into our favour!" project. The authors acknowledge the funding from "Technology development for healthy and safe protein during biorefinery" financed by the Wageningen Knowledge Base funds (KB37-004-009 and KB37-004-036) of Wageningen UR.

Declaration of competing interest

The authors declare that they have no known competing financial interests or personal relationships that could have appeared to influence the work reported in this paper.

Acknowledgement

The authors want to thank Edwin Bakx and Rene Kuijpers (Wageningen University) for assisting in MALDI-TOF-MS and SEC measurements; Gijs Vreeke, Jean-Paul Vincken, Atze Jan van der Goot, (Wageningen University); Marieke Bruin, and Maaike Nieuwland (Wageningen Food & Biobased Research) for insightful discussions; Janniek Ritsema (Wageningen University) for assistance with MOE computations; and Dominique Armbruster (Max Rubner-Institut) for assistance with QCM-D measurements. Part of the presented results were obtained using an ÄKTA pure 25 liquid chromatography system and an autoflex maX MALDI-TOF mass spectrometer, which are owned by WUR-Shared Research Facilities. Investment by WUR-Shared Research Facility was made possible by the 'Regio Deal Foodvalley'.

Appendix A. Supplementary data

Supplementary data to this article can be found online at https://doi.org/10.1016/j.foodhyd.2025.112405.

Data availability

Data will be made available on request.

References

Abd El-Maksoud, A. A., Abd El-Ghany, I. H., El-Beltagi, H. S., Anankanbil, S., Banerijee, C., Petersen, S. V., Pérez, B., & Guo, Z. (2018). Adding functionality to milk-based protein: Preparation, and physico-chemical characterization of β-lactoglobulin-phenolic conjugates. *Food Chemistry, 241*, 281–289. https://doi.org/10.1016/j.foodchem.2017.08.101

Ali, M., Keppler, J. K., Coenye, T., & Schwarz, K. (2018). Covalent whey protein–rosmarinic acid interactions: a comparison of alkaline and enzymatic modifications on physicochemical, antioxidative, and antibacterial properties. *Journal of Food Science, 83*(8), 2092–2100.

Anantharamkrishnan, V., & Reineccius, G. A. (2020). Method to characterize and monitor covalent interactions of flavor compounds with β-lactoglobulin using mass spectrometry and proteomics. *Journal of Agricultural and Food Chemistry, 68*(46), 13121–13130. https://doi.org/10.1021/acs.jafc.9b07978

Barth, A. (2007). Infrared spectroscopy of proteins. *Biochimica et Biophysica Acta - Bioenergetics, 1767*(9), 1073–1101. https://doi.org/10.1016/j.bbabio.2007.06.004

Çanak-Ipek, T., Girbas, M. G., Casadei, N., Schlensak, C., Marel, A.-K., & Avci-Adali, M. (2025). Development of a QCM-D-based aptasensor for the real-time detection of β-lactoglobulin. *Biosensors, 15*(9), 563. https://doi.org/10.3390/bios15090563

Cheynier, V. (2012). Phenolic compounds: From plants to foods. *Phytochemistry Reviews, 11*(2–3), 153–177. https://doi.org/10.1007/s11101-012-9242-8

Cilliers, J. J. L., & Singleton, V. L. (1991). Characterization of the products of nonenzymatic autoxidative phenolic reactions in a caffeic acid model system. *Journal of Agricultural and Food Chemistry, 39*(7), 1298–1303.

Condict, L., Kaur, J., Hung, A., Ashton, J., & Kasapis, S. (2019). Combined spectroscopic, molecular docking and quantum mechanics study of β-casein and ferulic acid interactions following UHT-like treatment. *Food Hydrocolloids, 89*, 351–359. https://doi.org/10.1016/j.foodhyd.2018.10.055

Delahaije, R. J. B. M., Gruppen, H., Van Eijk-Van Boxtel, E. L., Cornacchia, L., & Wierenga, P. A. (2016). Controlling the ratio between native-like, non-native-like, and aggregated β-lactoglobulin after heat treatment. *Journal of Agricultural and Food Chemistry, 64*(21), 4362–4370. https://doi.org/10.1021/acs.jafc.6b00816

Deng, Z., Xia, Y., Chen, L., Zhao, Y., Wang, R., & Liang, G. (2023). Insight into covalent conjugates of β-lactoglobulin with rutin: Characterizing allergenicity, digestibility, and antioxidant properties in vitro. *Food Research International, 173*. https://doi.org/10.1016/j.foodres.2023.113401

Dong, A., Randolph, T. W., & Carpenter, J. F. (2000). Entrapping intermediates of thermal aggregation in α-helical proteins with low concentration of guanidine hydrochloride. *Journal of Biological Chemistry, 275*(36), 27689–27693. https://doi.org/10.1074/jbc.M005374200

Drucker, C. T., Cicali, A. R., Roberts, A. M. P., Hughey, C. A., & Senger, L. W. (2023). Identification of alkaline-induced thiolyl-chlorogenic acid conjugates with cysteine and glutathione. *Food Chemistry, 423*. https://doi.org/10.1016/j.foodchem.2023.136267

Ersöz, N., & Dudak, F. C. (2020). The interaction between β-lactoglobulin and allyl-isothiocyanate. *Food Bioscience, 36*. https://doi.org/10.1016/j.fbio.2020.100600

Görner, A., Franz, L., Çanak-Ipek, T., Avci-Adali, M., & Marel, A. K. (2024). Development of an aptamer-based QCM-D biosensor for the detection of thrombin using supported lipid bilayers as surface functionalization. *Biosensors, 14*(6). https://doi.org/10.3390/bios14060270

Heyn, T. R., Garamus, V. M., Neumann, H. R., Uttinger, M. J., Guckeisen, T., Heuer, M., Selhuber-Unkel, C., Peukert, W., & Keppler, J. K. (2019). Influence of the polydispersity of pH 2 and pH 3.5 beta-lactoglobulin amyloid fibril solutions on analytical methods. *European Polymer Journal, 120*. https://doi.org/10.1016/j.eurpolymj.2019.08.038

Jia, Y., Yan, X., Huang, Y., Zhu, H., Qi, B., & Li, Y. (2022). Different interactions driving the binding of soy proteins (7S/11S) and flavonoids (quercetin/rutin): Alterations in the conformational and functional properties of soy proteins. *Food Chemistry, 396*. https://doi.org/10.1016/j.foodchem.2022.133685

Kalli, S., Araya-Cloutier, C., Chapman, J., Sanders, J. W., & Vincken, J. P. (2022). Prenylated (iso)flavonoids as antifungal agents against the food spoiler *Zygosaccharomyces parabailii*. *Food Control, 132*. https://doi.org/10.1016/j.foodcont.2021.108434

Kallinich, C., Schefer, S., & Rohn, S. (2018). Analysis of protein-phenolic compound modifications using electrochemistry coupled to mass spectrometry. *Molecules, 23*(2). https://doi.org/10.3390/molecules23020264

Kanakis, C. D., Hasni, I., Bourassa, P., Tarantilis, P. A., Polissiou, M. G., & Tajmir-Riahi, H. A. (2011). Milk β-lactoglobulin complexes with tea polyphenols. *Food Chemistry, 127*(3), 1046–1055. https://doi.org/10.1016/j.foodchem.2011.01.079

Kehoe, J. J., Brodkorb, A., Mollé, D., Yokoyama, E., Famelart, M. H., Bouhallab, S., Morris, E. R., & Croguennec, T. (2007). Determination of exposed sulfhydryl groups in heated β-lactoglobulin a using IAEDANS and mass spectrometry. *Journal of Agricultural and Food Chemistry, 55*(17), 7107–7113. https://doi.org/10.1021/jf070397r

Keppler, J. K., Koudelka, T., Palani, K., Stuhldreier, M. C., Temps, F., Tholey, A., & Schwarz, K. (2014). Characterization of the covalent binding of allyl isothiocyanate to β-lactoglobulin by fluorescence quenching, equilibrium measurement, and mass spectrometry. *Journal of Biomolecular Structure and Dynamics, 32*(7), 1103–1117. https://doi.org/10.1080/07391102.2013.809605

Keppler, J. K., Koudelka, T., Palani, K., Tholey, A., & Schwarz, K. (2014). Interaction of β-lactoglobulin with small hydrophobic ligands - Influence of covalent AITC modification on β-LG tryptic cleavage. *Food Biophysics, 9*(4), 349–358. https://doi.org/10.1007/s11483-014-9361-4

Keppler, J. K., Martin, D., Garamus, V. M., Berton-Carabin, C., Nipoti, E., Coenye, T., & Schwarz, K. (2017). Functionality of whey proteins covalently modified by allyl isothiocyanate. Part 1 physicochemical and antibacterial properties of native and modified whey proteins at pH 2 to 7. *Food Hydrocolloids, 65*, 130–143. https://doi.org/10.1016/j.foodhyd.2016.11.016

Keppler, J. K., & Schwarz, K. (2017). Increasing the emulsifying capacity of whey proteins at acidic pH values through covalent modification with allyl isothiocyanate. *Colloids and Surfaces A: Physicochemical and Engineering Aspects, 522*, 514–524. https://doi.org/10.1016/j.colsurfa.2017.03.033

Keppler, J. K., Schwarz, K., & van der Goot, A. J. (2020). Covalent modification of food proteins by plant-based ingredients (polyphenols and organosulphur compounds): A commonplace reaction with novel utilization potential. *Trends in Food Science and Technology, 101*, 38–49. https://doi.org/10.1016/j.tifs.2020.04.023

Keppler, J. K., Sönnichsen, F. D., Lorenzen, P. C., & Schwarz, K. (2014). Differences in heat stability and ligand binding among β-lactoglobulin genetic variants A, B and C using ^{1}H NMR and fluorescence quenching. *Biochimica et Biophysica Acta - Proteins and Proteomics, 1844*(6), 1083–1093. https://doi.org/10.1016/j.bbapap.2014.02.007

Keppler, J. K., Van der Goot, A. J., & Reineccius, G. (2024). Hydrophobic/hydrophilic surface activity III: Interactions with other micro- and macromolecules. In *Functionality of plant proteins: Properties, methods of assessment, modifications and applications* (pp. 197–220). Elsevier. https://doi.org/10.1016/B978-0-323-91721-6.00004-9.

Kieserling, H., de Bruijn, W. J. C., Keppler, J., Yang, J., Sagu, S. T., Güterbock, D., Rawel, H., Schwarz, K., Vincken, J. P., Schieber, A., & Rohn, S. (2024). Protein–phenolic interactions and reactions: Discrepancies, challenges, and opportunities. *Comprehensive Reviews in Food Science and Food Safety, 23*(5). https://doi.org/10.1111/1541-4337.70015

Kong, X., Huang, Z., Zhang, C., Hua, Y., Chen, Y., & Li, X. (2023). Phenolic compounds in walnut pellicle improve walnut (*Juglans regia* L.) protein solubility under pH-shifting condition. *Food Research International, 163*. https://doi.org/10.1016/j.foodres.2022.112156

Li, D., Wang, R., Ma, Y., & Yu, D. (2023). Covalent modification of (+)-catechin to improve the physicochemical, rheological, and oxidative stability properties of rice bran protein emulsion. *International Journal of Biological Macromolecules, 249*. https://doi.org/10.1016/j.ijbiomac.2023.126003

Li, D., Zhu, L., Wu, Q., Chen, Y., Wu, G., & Zhang, H. (2024). Tartary buckwheat protein-phenol conjugate prepared by alkaline-based environment: Identification of covalent binding sites of phenols and alterations in protein structural and functional characteristics. *International Journal of Biological Macromolecules, 257*. https://doi.org/10.1016/j.ijbiomac.2023.127504

Liu, J., Engholm-Keller, K., Poojary, M. M., Bevilacqua, M., Andersen, M. L., & Lund, M. N. (2024). Reactivity and mechanism of the reactions of 4-methylbenzoquinone with amino acid residues in β-lactoglobulin: A kinetic and product investigation. *Food Chemistry, 434*. https://doi.org/10.1016/j.foodchem.2023.137473

Liu, J., Wang, Q., Zhang, H., Yu, D., Jin, S., & Ren, F. (2016). Interaction of chlorogenic acid with milk proteins analyzed by spectroscopic and modeling methods. *Spectroscopy Letters, 49*(1), 44–50. https://doi.org/10.1080/00387010.2015.1066826

Lund, M. N. (2021). Reactions of plant polyphenols in foods: Impact of molecular structure. In *Trends in food science and technology, 112* pp. 241–251). Elsevier Ltd. https://doi.org/10.1016/j.tifs.2021.03.056.

Malik, M. A., Sharma, H. K., & Saini, C. S. (2016). Effect of removal of phenolic compounds on structural and thermal properties of sunflower protein isolate. *Journal of Food Science and Technology, 53*(9), 3455–3464. https://doi.org/10.1007/s13197-016-2320-y

Man, P., Sun, L., Han, X., Zhang, H., Qin, L., & Ren, H. (2024). Effects of different tea polyphenols conjugated with β-lactoglobulin on antioxidant capacity and structural properties. *LWT, 198*. https://doi.org/10.1016/j.lwt.2024.115990

Masoumi, B., Tabibiazar, M., Golchinfar, Z., Mohammadifar, M., & Hamishehkar, H. (2024). A review of protein-phenolic acid interaction: Reaction mechanisms and applications. In *Critical reviews in food science and nutrition, 64* pp. 3539–3555). Taylor and Francis Ltd. https://doi.org/10.1080/10408398.2022.2132376, 11.

Muzolf-Panek, M., Gliszczyńska-Świgło, A., Szymusiak, H., & Tyrakowska, B. (2012). The influence of stereochemistry on the antioxidant properties of catechin epimers. *European Food Research and Technology, 235*(6), 1001–1009. https://doi.org/10.1007/s00217-012-1826-4

Ozdal, T., Capanoglu, E., & Altay, F. (2013). A review on protein-phenolic interactions and associated changes. *Food Research International, 51*, 954–970. https://doi.org/10.1016/j.foodres.2013.02.009

Pang, X. H., Yang, Y., Bian, X., Wang, B., Ren, L. K., Liu, L. L., Yu, D. H., Yang, J., Guo, J. C., Wang, L., Zhang, X. M., Yu, H. S., & Zhang, N. (2021). Hemp (*Cannabis sativa* l.) seed protein–EGCG conjugates: Covalent bonding and functional research. *Foods, 10*(7). https://doi.org/10.3390/foods10071618

Parolia, S., Maley, J., Sammynaiken, R., Green, R., Nickerson, M., & Ghosh, S. (2022). Structure – Functionality of lentil protein-polyphenol conjugates. *Food Chemistry, 367*. https://doi.org/10.1016/j.foodchem.2021.130603

Pritchard, H. O., & Skinner, H. A. (1955). The concept of electronegativity. *Chemical Reviews, 4*, 745–786. https://pubs.acs.org/sharingguidelines.

Pu, P., Deng, Z., Chen, L., Yang, H., & Liang, G. (2023). Reducing antigenicity and improving antioxidant capacity of β-lactoglobulin through covalent interaction with six flavonoids. *Foods, 12*(15). https://doi.org/10.3390/foods12152913

Rade-Kukic, K., Schmitt, C., & Rawel, H. M. (2011). Formation of conjugates between β-lactoglobulin and allyl isothiocyanate: Effect on protein heat aggregation, foaming and emulsifying properties. *Food Hydrocolloids, 25*(4), 694–706. https://doi.org/10.1016/j.foodhyd.2010.08.018

Rawel, H. M., Czajka, D., Rohn, S., & Rgen Kroll, J. (2002). Interactions of different phenolic acids and flavonoids with soy proteins. *International Journal of Biological Macromolecules, 30*(3–4), 137–150. https://doi.org/10.1016/S0141-8130(02)00016-8

Rawel, H. M., Kroll, J., & Hohl, U. C. (2001). Model studies on reactions of plant phenols with whey proteins. *Nahrung-Food, 45*(2), 72–81. https://doi.org/10.1002/1521-3803(20010401)45:2<72::AID-FOOD72>3.0.CO;2-U

Rohn, S. (2014). Possibilities and limitations in the analysis of covalent interactions between phenolic compounds and proteins. *Food Research International, 65*, 13–19. https://doi.org/10.1016/j.foodres.2014.05.042

Schröder, A., Berton-Carabin, C., Venema, P., & Cornacchia, L. (2017). Interfacial properties of whey protein and whey protein hydrolysates and their influence on O/W emulsion stability. *Food Hydrocolloids, 73*, 129–140. https://doi.org/10.1016/j.foodhyd.2017.06.001

Sęczyk, L., Świeca, M., Kapusta, I., & Gawlik-Dziki, U. (2019). Protein–phenolic interactions as a factor affecting the physicochemical properties of white bean proteins. *Molecules, 24*(3), 408. https://doi.org/10.3390/molecules24030408

Stănciuc, N., Râpeanu, G., Bahrim, G. E., & Aprodu, I. (2020). The interaction of bovine β-lactoglobulin with caffeic acid: From binding mechanisms to functional complexes. *Biomolecules, 10*(8), 1–14. https://doi.org/10.3390/biom10081096

Tanger, C., Engel, J., & Kulozik, U. (2020). Influence of extraction conditions on the conformational alteration of pea protein extracted from pea flour. *Food Hydrocolloids, 107*. https://doi.org/10.1016/j.foodhyd.2020.105949

Wang, Y., Zhang, P., Lin, H., Fei, X., Zhang, G., & Hu, X. (2024). Covalent binding of β-lactoglobulin and rosmarinic acid by alkaline and free-radical treatment: Improved thermal stability and antioxidant capability. *Food Bioscience, 61*. https://doi.org/10.1016/j.fbio.2024.104574

Xu, C., & Chen, X. (2011). Molecular property-affinity relationship of the interaction between dietary polyphenols and bovine milk proteins. *Food & Function, 2*(7), 368–372. https://doi.org/10.1039/c1fo10074b

Xue, Y. T., Han, Y. N., Wang, Y., Zhang, Y. H., Yin, Y. Q., Liu, B. H., Zhang, H. L., & Zhao, X. H. (2023). Effect of ferulic acid covalent conjugation on the functional properties and antigenicity of β-lactoglobulin. *Food Chemistry, 406*. https://doi.org/10.1016/j.foodchem.2022.135095

Yan, X., Chu, Y., Hang, J., Zhang, S., Yu, P., Gong, X., Zeng, Z., & Chen, L. (2024). Enhancing emulsifying properties of lentil protein fibrils through EGCG mediation and the mechanism study. *Food Hydrocolloids, 153*. https://doi.org/10.1016/j.foodhyd.2024.109972

Yan, S., Yao, Y., Xie, X., Zhang, S., Huang, Y., Zhu, H., Li, Y., & Qi, B. (2022). Comparison of the physical stabilities and oxidation of lipids and proteins in natural and polyphenol-modified soybean protein isolate-stabilized emulsions. *Food Research International, 162*. https://doi.org/10.1016/j.foodres.2022.112066

Ye, J., Deng, L., Wang, Y., McClements, D. J., Luo, S., & Liu, C. (2021). Impact of rutin on the foaming properties of soybean protein: Formation and characterization of flavonoid-protein complexes. *Food Chemistry, 362*. https://doi.org/10.1016/j.foodchem.2021.130238

Zhang, Q., Cheng, Z., Wang, Y., & Fu, L. (2021). Dietary protein-phenolic interactions: Characterization, biochemical-physiological consequences, and potential food applications. *Critical Reviews in Food Science and Nutrition, 61*(21), 3589–3615. https://doi.org/10.1080/10408398.2020.1803199

Zhou, X., Iqbal, A., Li, J., Liu, C., Murtaza, A., Xu, X., Pan, S., & Hu, W. (2021). Changes in browning degree and reducibility of polyphenols during autoxidation and enzymatic oxidation. *Antioxidants, 10*(11). https://doi.org/10.3390/antiox10111809